Targeting PP2A with lomitapide suppresses colorectal tumorigenesis through the activation of AMPK/Beclin1-mediated autophagy

Qian Zuo
Jinan University
Long Liao
Jinan University
Ziting Yao
Jinan University
Yaping Liu
Jinan University
Dingkang Wang
Jinan University
Shujun Li
Jinan University
Xingfeng Yin
Jinan University
Qingyu He
Jinan University
Wenwen Xu (xuwen6966@163.com)
Jinan University

Research

Keywords: Lomitapide, Colorectal cancer, PP2A inhibitor, AMPK, autophagy

Posted Date: June 4th, 2021

DOI: https://doi.org/10.21203/rs.3.rs-573782/v1

Abstract

Background

Colorectal cancer (CRC) is one of the most malignant cancer worldwide, and the limited efficacy of existing treatments is the leading cause of death in patients with CRC. Thus, novel drugs for CRC treatment are urgently needed.

Methods

We screened an FDA-approved small-molecule library upon HCT116 cells, and identified lomitapide as a novel CRC anticancer compound. Then we confirmed the activities of lomitapide on CRC cells by WST-1 assay, colony formation, and flow cytometry. RNA sequencing and GO analysis were used to investigate the mechanisms underlying the anticancer effects of lomitapide. LiP-SMap was introduced to search for the potential targets of lomitapide. The in vivo experiment was conducted to confirm the therapeutic efficiency and safety of lomitapide as an anticancer agent.

Results

Lomitapide exhibited remarkable antitumor properties *in vitro* and *in vivo*, while activated autophagy is characterized by GO analysis as a key biological process in lomitapide-induced CRC repression. Moreover, lomitapide stimulated mitochondrial dysfunction-mediated AMPK activation, resulting in increased AMPK phosphorylation and enhanced Beclin1/Atg14/Vps34 interactions, provoking autophagy induction. LiP-SMap analysis showed that PP2A was the direct target of lomitapide, and the bioactivity of lomitapide was attenuated in PP2A-deficient cells, suggesting that the anticancer effect of lomitapide occurs in a PP2A-dependent manner.

Conclusions

Our results indicate that lomitapide activates AMPK-regulated autophagy to inhibit the proliferation and tumorigenesis of CRC cells by directly targeting PP2A, and can be a novel therapeutic agent for the treatment of CRC patients.

Background

Colorectal cancer (CRC) is the third leading cause of cancer mortality worldwide. With advances in diagnostic techniques and therapeutic strategies, the survival time for patients with CRC has increased in recent decades, yet the mortality rate of CRC remains high due to limited efficacy and significant side effects of treatments [1]. Hence, novel drugs for CRC treatment are urgently needed. Currently, drug repurposing has gradually emerged as an alternative approach to cancer treatment. This is a promising

strategy for investigating novel antineoplastic medicines,because it capitalizes on previous investments while derisking clinical trials. In this study, a drug library consisting of 1056 U.S. Food and Drug Administration (FDA)-approved medications was tested for compounds with anticancer indications. Lomitapide, an inhibitor of mitochondrial trifunctional protein (MTP), which is usually used for the treatment of hypercholesterolemia in the clinic [2], was found to significantly suppress colorectal tumorigenesis. To the best of our knowledge, the anticancer properties of lomitapide have not been reported, and the mechanism involved is not clear.

Autophagy is an evolutionarily conserved process that maintains cellular metabolism and homeostasis [3] and is subjected to a range of cellular stresses, including oxidative stress, mitochondrial abnormalities and abnormal protein accumulation [4–6]. Several studies have indicated that autophagy can act to suppress tumor survival and growth in advanced cancers [7]. In addition, silencing of some key autophagy-related genes has been reported to facilitate tumor progression in colon, gastric, breast, and prostate cancers [8–10]. However, the regulatory role of autophagy in colorectal tumorigenesis remains ambiguous. Many studies have revealed that the modulation of autophagy by the mTOR, AMPK, and MAPK pathways plays a critical role in CRC [11–13]. Targeting autophagy via key signaling pathways has been recognized as an effective approach to CRC therapy. In this study, RNA sequencing was performed with lomitapide-treated CRC cells, and pathway enrichment analyses of differentially expressed genes suggested that autophagy activation may contribute to the antitumor effects of lomitapide. The direct target of lomitapide in cancer cells is important to its clinical implications but remains to be elucidated.

Quantitative proteomic analysis coupled with bioinformatics analysis has been identified as a favorable strategy for exploring the molecular mechanism underlying the actions of small molecules [14]. In previous studies, we successfully used drug affinity responsive target stability (DARTS) technology to demonstrate that ADP-ribosylation factor 1 (ARF1) acts as a direct target and mediates the anticancer effect of azelastine [15]. In contrast to DARTS technology, the optimized limited proteolysis-mass spectrometry (LiP-SMap) method takes advantage of high-resolution LC-MS/MS and high-throughput quantitative proteomic technology to identify increased peptide levels upon limited proteolysis. Moreover, LiP-SMap relies on the binding affinity between a small molecule and its target protein(s), providing more consistent peptide detection and accurate proteome quantification [16]. Here, by performing an optimized LiP-SMap, we found that protein phosphatase 2A (PP2A), which plays a crucial role in various biological processes [17], is a direct target of lomitapide in cancer cells. Although PP2A was originally characterized as a tumor suppressor, recent studies have revealed that targeting PP2A can achieve therapeutic benefits in certain malignancies via cell cycle arrest, apoptosis induction and disruption of DNA repair [18–20]. In the present study, a series of functional assays were performed to investigate whether lomitapide activates AMPK-regulated autophagy to inhibit the proliferation and tumorigenesis of CRC cells by directly targeting PP2A.

Methods

Drugs, antibodies and reagents

Lomitapide was acquired from Selleck Chemicals (Huston, TX, USA) and freshly prepared into 5 mM stock solution with DMSO. Anti-Caspase-3, anti-cleaved caspase-3, anti-cleaved PARP, anti-LC3B, anti-AMPKα, anti-phospho-AMPKα Thr172, anti-phospho-Beclin-1 Ser93, and anti-Beclin-1 antibodies were purchased from Cell Signaling Technology (Danvers, MA, USA). Anti-Vps34, anti-Atg14 and anti-Gapdh antibodies were obtained from Proteintech (Chicago, IL, USA). The WST-1 cell proliferation and cytotoxicity assay kit, glutathione S-transferase (GST) tag protein purification kit, reactive oxygen species assay kit and PreScission protease were obtained from Beyotime Biotechnology (Shanghai, China). An Annexin V-FITC/PI apoptosis detection kit was obtained from KeyGen Biotechnology (Nanjing, Jiangsu, China). Protein A/G PLUS-agarose was purchased from Santa Cruz Biotechnology (Santa Cruz, CA, USA).

Cell culture

The HCT116 and HT29 human colorectal cancer cell lines were obtained from American Type Culture Collection (ATCC, Rockville, MD, USA). The cells were routinely maintained in DMEM (Thermo Fisher Scientific, San Jose, CA, USA) supplemented with 10% fetal bovine serum and penicillin and streptomycin at 37 °C in 5% CO_2.

RNA interference and CRISPR-Cas9-KO cell lines

The siRNAs against human AMPKα were obtained from TranSheepBio (Shanghai, China), and the sequences were 5’-GCUAUCUUCUGGACUUCAA-3’ for siAMPK#1 and 5’-ACCAUGAUUGAUGAUGAAGCCUUAA-3’ for siAMPK#2. To establish stable cell lines with PP2A knocked out, we selected effective sgRNA sequences for PP2A knockout with Clustered Regularly Interspaced Short Palindromic Repeats (CRISPR)/CRISPR-associated protein 9 (Cas9) technology [21]. The sequence of sgRNA against PP2A was 5’- GAAGCTGTCCACCATCGCCT -3’. Briefly, 293T cells were cotransfected with the indicated expression vectors and virus skeleton vectors by using Lipofectamine 3000 (Thermo Fisher Scientific, San Jose, CA, USA). HCT116 and HT29 cells were infected with lentiviral supernatants, and were selected with 5 μg/mL puromycin. Successful gene knockout was confirmed by immunoblot analysis.

Cell proliferation assays

Cells were exposed to lomitapide at indicated concentrations for 24 h, 48 h, and 72 h. The cell viabilities were assessed by WST-1 assay (Beyotime Biotechnology, Shanghai, China) according to the

manufacturer's instructions [22]. The results were obtained by measuring the absorbance with an automated microplate spectrophotometer (BioTek Instruments, Winooski, VT, USA) at 490 nm.

Colony formation assay

To analyze long-term survival, HCT116 and HT29 cells at a density of 500 or 800 cells per well were seeded in 6-well plates, and treated with lomitapide for 14 days. The colonies were fixed with 75% ethanol, stained with 1% crystal violet, and counted for analysis.

Flow cytometric analysis

The cell apoptosis was detected using an Annexin V-FITC/PI apoptosis detection kit, and analyzed by a BD FACSCelesta flow cytometer (BD Biosciences, San Diego, CA). For intracellular ROS level measurement, cells were stained with 10 μM dichloro-dihydro-fluorescein diacetate (DCFH-DA) dye in serum-free culture medium at 37 °C for 20 min in the dark and washed with PBS, and the relative DCFH fluorescence of the cells was analyzed with a BD FACSCelesta flow cytometer.

ATP production assay

For measurements of ATP levels, cell lysates were centrifuged at 12,000 g for 5 min, and the supernatant was mixed with an ATP working dilution (Beyotime Biotechnology). Luminance was measured using a monochromator microplate reader.

Immunofluorescence (IF) staining

Laser scanning confocal microscopy (Carl Zeiss AG, Jena, Thuringia, Germany) was carried out as reported previously [23]. In brief, the lomitapide-treated or control cells were fixed with 4% paraformaldehyde, permeabilized with 0.1% TrintonX-100, and blocked with 5% blocking buffer. Then cells were stained with anti-LC3B antibody, and counterstained with DAPI (Thermo Fisher Scientific, Waltham, MA, USA). Images were visualized and pictures in the same panel were taken under the same excitation conditions.

Detection of mitochondrial morphology

Morphology of mitochondria was determined with the MitoTracker Mitochondrion-Selective Probe (Invitrogen, Gaithersburg, MD, USA). Cells were incubated with the MitoTracker® probe (100 nM) for 30 min at room temperature, and fixed with 4% formaldehyde and then stained with DAPI. Confocal microscopy was performed and the obtained images were analyzed by ImageJ software with the mitochondrial network analysis (MiNA) toolset.

Coimmunoprecipitation and immunoblotting

For coimmunoprecipitation (co-IP) assay, HCT116 and HT29 cells were transfected with the indicated plasmids for 24 h, following by the lomitapide treatment for another 48 h. The collected cells were lysed with ice-cold RIPA buffer containing 2% phenylmethyl sulfonyl fluoride and 10% phosphatase inhibitor for 40 min. After centrifugation for 30 min at 134,000 g at 4 °C, about 10% of the supernatant was collected as input, and the rest cell lysate was incubated with the indicated antibodies overnight at 4 °C. Then cell lysate was incubated with Protein A/G plus agarose at 4 °C for 4 h, and washed with lysis buffer 5 times. The immunoprecipitated proteins were detected by Western blot analysis and visualized with the enhanced chemiluminescent (ECL) reagent (Bio-Rad, Hercules, CA, USA). The images were obtained using a Tanon 5200 Multi chemiluminescent imaging system (Tanon Science & Technology Co. Ltd., Shanghai, China).

Protein expression and purification

The pGEX-4T-1 vector was used to construct the pGEX-4T-1-PP2A plasmids expressing (GST)-tagged PP2A fusion proteins, as previously described [24]. The expression plasmids were transformed into *Escherichia coli* BL21, and the cells grown in LB medium at 37 °C until the optical density reached 0.6–0.8 at 600 nm. To induce target protein expression, 0.5 mM isopropyl-β-d-thiogalactoside (IPTG) was added to the LB medium and cultured with the bacteria for an additional 12 h at 20 °C. Bacteria were then harvested, resuspended in binding buffer (20 mM Na3PO4·12 H_2O and 0.5 M NaCl, Ph = 7.4) and sonicated for 20 min followed by centrifugation at 12,000 g for 30 min. GST-affinity column (Glutathione Sepharose 4B, GE Healthcare) was used to collect the protein with GST-tag. After washing with elution buffer (10 mM GSH and 50 mM Tris-HCl) thoroughly, the target protein was harvested with a centrifugal filter (10 K, Merck Millipore). Afterwards, the GST-tag was removed by overnight digestion with thrombin (GE Healthcare) at room temperature.

Surface plasmon resonance (SPR)

SPR was conducted on an OpenSPR system (Nicoya Lifesciences Inc., Kitchener, Canada) to evaluate the binding affinity of lomitapide to PP2A. In brief, protein was immobilized on sensor chips, and lomitapide

solution was introduced into the sensor chip.

Nude mice xenograft model

The animal study in this research was approved by the Ethics Committee for Animal Experiments of Jinan University. Tumor-bearing mice were established by subcutaneous injection of 2 x 10^6 HT29 cells suspended in a 1:1 mixture of PBS: Matrigel (Corning Incorporated, Tewksbury, MA, USA). The mice were treated with 20 mg/kg lomitapide or vehicle by gavage, every two days. The tumor volume were measured every 3 days with the formula: $V = 0.5 \times \text{length} \times \text{width}^2$. At the end of the experiment, tumors were harvested for TUNEL assay and Ki67 staining, together with livers, kidneys, and lungs were collected for histologic analyses.

Statistical analysis

All *in vitro* experiments were performed in triplicate. Two-tailed Student's tests, one-way ANOVA, two-way ANOVA, and Chi-square test were performed using GraphPad Prism software v.5.01 (San Diego, CA, USA). All values were expressed as the means ± SD, and $P < 0.05$ was considered statistically significant.

Results

3.1 Screening of an FDA-approved small-molecule library led to the identification of lomitapide as a novel CRC anticancer compound

To obtain novel anti-cancer agents, a drug library of 1056 FDA-approved medications was tested for antitumor effects. HCT116 cells were intervened with the 1056 compounds individually at an identical concentration of 10 μM for 48 h, and the inhibitory effects of small-molecules on cells were evaluated by WST-1 assay. As shown in Fig. 1a, lomitapide, an agent widely used for treating hypercholesterolemia, was one of the most potent compounds in suppressing the proliferation of HCT116 cells, indicating that it may be a potential anticancer agent.

To further validate whether lomitapide exerts antitumor actions against CRC, we firstly tested the cell viabilities of different human CRC cell lines post lomitapide treatment. As shown in Fig. 1b, lomitapide significantly decreased the growth rate of the HCT116 and HT29 CRC cell lines. The *in vitro* tumorigenicity of these CRC cells was significantly impaired under lomitapide treatment, as verified by the reduced colony formation in the lomitapide-treated cells (Fig. 1c). To investigate whether apoptosis is involved in lomitapide-induced suppression of CRC cells viabilities, we conducted flow cytometry assays and detected obvious apoptotic CRC cells resulting from lomitapide treatment (Fig. 1d). In addition, lomitapide treatment led to increased levels of cleaved caspase-3 and cleaved PARP in the CRC cells (Fig.

1e). Collectively, the above results implied that lomitapide may exert anticancer effect in CRC cells *in vitro*.

3.2 Autophagy induction contributes to the antitumor activity of lomitapide in CRC cells

Accumulating evidence has highlighted the potential implication of autophagy-regulating drugs for use in cancer therapy [25, 26]. In this study, RNA sequencing (RNA-seq) was used to compare the gene profiles of lomitapide-treated CRC cells and control cells, and pathway enrichment analysis of the differentially expressed genes in lomitapide-treated cells suggested that the anticancer effect of lomitapide in CRC cells may be attributed to autophagy activation (Fig. 2a). In order to investigate the regulatory role of lomitapide on autophagy in CRC cells, western blot data showed that lomitapide treatment not only facilitated the turnover of LC3-I to LC3-II, but also augmented the accumulation of autophagic vesicles (LC3 puncta) in a dose-dependent manner (Fig. 2b, Supplementary Figure S1a).

To investigate the crucial role of autophagy in the anticancer effect of lomitapide, bafilomycin A1 (Baf-A1), an autophagy inhibitor, was applied to CRC cells. As shown in Supplementary Figure S1b, Baf-A1 restored lomitapide-induced cell proliferation inhibition. A similar increase in cell proliferation was also detected in lomitapide-treated CRC cells coupled with Baf-A1, as further validated by colony formation assay (Fig. 2c). Moreover, the increased apoptosis rate, as well as the apoptotic proteins, of lomitapide-treated CRC cells was markedly attenuated by Baf-A1 treatment (Fig. 2d, Supplementary Figure S1c). Taken together, these data demonstrated that lomitapide may have exerted its anticancer actions in the CRC cells through activation of autophagy.

3.3 Lomitapide triggers AMPK-regulated autophagy through mitochondrial ATP depletion and ROS accumulation in CRC cells

Mitochondrial fission and fusion play critical roles in maintaining functional mitochondria, while the disruption of mitochondrial dynamics leads to altered mitochondrial morphology, increased amounts of ROS and a decreased ATP synthesis rate, thus fueling autophagy [27, 28]. To investigate whether lomitapide-induced autophagy is attributable to mitochondrial dysfunction, we performed immunofluorescence staining to detect the morphology of the mitochondrial network, and an obviously higher ratio of tubular mitochondria was observed in lomitapide-treated HCT116 and HT29 cells, implying the disruption of mitochondrial balance by lomitapide (Fig. 3a). This finding was confirmed by reduced ATP levels and enhanced ROS levels in lomitapide-treated CRC cells (Fig. 3b and 3c). We proposed that the impaired mitochondrial dynamics induced by lomitapide contribute to the activation of autophagy in CRC cells; however, the molecular mechanisms involved remain unclear.

Since various mitochondrial signals, including ATP levels and ROS production, can activate AMPK [29-31], we next examined whether AMPK may respond to the indicated stressors arising from lomitapide-induced mitochondrial dysfunction. The results showed that p-AMPK and p-ACC were upregulated in lomitapide-treated CRC cells (Fig. 3d). The mechanism underlying the effect of lomitapide on AMPK-regulated autophagy was further studied. Since AMPK has been reported to phosphorylate multiple tyrosine sites of

Beclin1, leading to enhanced association of Beclin1 with pro-autophagy proteins such as Vps34 and Atg14[32, 33], we postulated that lomitapide might facilitate the formation of the Beclin1-Atg14-Vps34 complex via AMPK signaling. To verify this assumption, we performed a coimmunoprecipitation assay to analyze the interaction of Beclin1 with other proteins in lomitapide-treated CRC cells. As shown in Fig. 3e, the interaction of Beclin1 with Atg14 and Vps34 was significantly enhanced in the presence of lomitapide. Collectively, these results revealed that mitochondrial dysfunction-mediated AMPK phosphorylation was required for lomitapide-induced autophagy in these CRC cells.

3.4 AMPK silencing impairs lomitapide-induced autophagic cell death

To validate whether activation of AMPK, not the modulation of other signaling pathways, accounts for the lomitapide-induced autophagic cell death of CRC cells, we examined the anticancer effect of lomitapide in AMPK-knockdown CRC cells. As shown in Fig. 4a-d, AMPK silencing profoundly counteracted the toxicity induced by lomitapide in HCT116 and HT29 cells, as evidenced by enhanced cell proliferation and reduced apoptosis rates. Moreover, the elevated number of autophagic vacuoles, as represented by the LC3-II levels and GFP-LC3 puncta in the lomitapide-treated CRC cells, was markedly abrogated when the cells were transfected with siRNAs against AMPK (Fig. 4e and Supplementary Figure S2e). Consistently, knockdown of AMPK attenuated the promoting effect of lomitapide on the formation of the Beclin1-Atg14-Vps34 complex. Taken together, these data suggested that AMPK/Beclin1-mediated autophagy was critical for lomitapide-induced CRC suppression (Fig. 4f).

3.5 Targeting PP2A decreases lomitapide-induced AMPK phosphorylation and CRC suppression.

To identify potential targets of lomitapide, LiP-SMap was introduced to search for the proteins that could directly bind to lomitapide. Among the candidate proteins, PP2A, a well-known upstream regulator of AMPK phosphorylation[34], drew our attention and became our focus in this study. We purified the PP2A protein, and the binding of lomitapide with PP2A was validated by surface plasmon resonance assay (Fig. 5b and 5c).

We proposed that PP2A may be a direct target for mediating AMPK-regulated cell death of lomitapide-treated CRC cells. To confirm this hypothesis, we generated PP2A-knockout HCT116 and HT29 cell lines (PP2A-KO) using the CRISPR/Cas9 system and observed that lomitapide failed to stimulate the phosphorylation of AMPK and ACC in the PP2A-deficient cells (Fig. 5d and 5e). Then, we further investigated whether lomitapide-induced cell death required PP2A-dependent activation of AMPK. As shown in Supplementary Figure S3a and Fig. 5f, PP2A knockout attenuated lomitapide-induced growth inhibition of the CRC cells, as presented by WST-1 and colony formation assays. Moreover, in contrast to the PP2A-expressing cell line (Figure 1d and 1e), moderate apoptosis rates of the HCT116-PP2A-KO and HT29-PP2A-KO cells exposed to lomitapide were observed (Fig. 5g and 5h). Collectively, these findings suggested that PP2A was important for lomitapide-induced p-AMPK upregulation and proliferation suppression in these CRC cells.

3.6 Lomitapide exhibits antitumor effects against CRC in vivo

As shown in Fig. 6a, mice treated with lomitapide exhibited a lower growth comparing to the vehicle-treated group mice. In addition, either tumor volumes or tumor weights were significantly reduced in the lomitapide-treated mice (Fig. 6b and 6c). Additionally, a TUNEL assay and Ki-67 immunohistochemical analysis were performed to detect apoptosis and proliferation indices. As indicated in Fig. 6d and 6f, xenografts from lomitapide-treated mice presented an increased cell apoptosis rate and decreased cell proliferation rate. Western blot data showed that lomitapide activated the AMPK pathway and autophagy in tumor tissues, indicated by increased expression levels of p-AMPK and LC3 I/II (Fig. 6h). Notably, the lomitapide treatment induced no toxic effect on the animals, as indicated by unchanged body weight and pathological morphology of major organs (Fig. 6e and 6g). Collectively, these results verified the therapeutic efficiency and safety of lomitapide as an anticancer agent.

Discussion

Autophagy has been extensively studied in cancers, and it is now universally recognized that autophagy has dual, contradictory roles in cancer progression [35]. Intracellular autophagy can be enhanced by a series of stressors, such as oxidative stress, nutrient starvation, and misfolded protein accumulation. Once the process is activated, a portion of the cytoplasm and organelles will enter the autophagic vesicles in succession, responding to the cellular stresses [36]. Owing to sustained autophagic stimulators, excessive autophagy leads to the depletion of organelles and key proteins and eventually leads to cell death [37–39]. Recently, several autophagy regulators, such as rapamycin, chloroquine, and hydroxychloroquine, have been widely used in cancer therapy [25, 40–43]. Thus, the development of novel autophagy regulators has presented remarkable potential in CRC treatment.

In recent years, drug repositioning strategies have gained considerable momentum, with approximately one-third of new drug approvals corresponding to repurposed drugs [44]. For example, metformin, a first-line medication for the treatment of type 2 diabetes, has been developed as an anti-cancer agent and is currently under phase II/phase III clinical trials [45]. A novel use of aspirin against prostate cancer has also been reported [46]. Our previous studies also identified several traditional drugs that exhibit potential anticancer actions [15, 22, 24, 47, 48]. In the present study, lomitapide, an inhibitor of MTP routinely applied in the management of hypercholesterolemia, was found to suppress CRC growth through activation of autophagy, further implying the significance of drug repurposing in the development of cancer therapy.

Our study provides the first evidence that lomitapide exhibits a strong antitumor effect against CRC cells, as validated by WST-1, colony formation and flow cytometry assays (Fig. 1). Lomitapide induces activation of AMPK by interfering with mitochondrial dynamics and intracellular ATP and ROS levels (Fig. 3). Mechanistically, our study demonstrates that lomitapide promotes the recruitment of the Beclin1-Atg14-Vps34 complex, which is required for autophagosome formation, thus inducing AMPK-regulated autophagy in colorectal cancer cells (Figs. 2 and 3). AMPK regulates autophagy by interacting with the Beclin1 complex. Phosphorylated AMPK participates in the direct phosphorylation of Beclin1 at multiple tyrosine sites, contributing to enhanced binding of Beclin1 with pro-autophagic proteins such as Vps34

and Atg14. Thus, formation of the Beclin1-Atg14-Vps34 complex is promoted, and autophagy is initiated [32, 49, 50]. Our results demonstrate that lomitapide-mediated interaction of Beclin1 with Vps34 and Atg14, as well as autophagy induction, is compromised by AMPK silencing. Furthermore, the anticancer property of lomitapide is abrogated in AMPK-knockdown CRC cells (Fig. 4). These results, therefore, indicate that the suppressive activity of lomitapide in CRC cells is dependent on AMPK/Beclin1-mediated autophagy.

Interestingly, our study also reveals that lomitapide can directly target PP2A, thus activating AMPK-regulated autophagy to inhibit CRC tumorigenesis. PP2A, an essential Ser/Thr phosphatase modulating numerous signaling pathways by dephosphorylating key components of these pathways [51–53] in cells, is involved in the regulation of a broad range of cancer hallmarks. It has also been reported that PP2A physically interacts with AMPK and reduces its activity via Thr172 dephosphorylation [54]. Another study indicated that nilotinib, a novel TKI, induced autophagic cell death in HCC via PP2A-regulated AMPK dephosphorylation [55]. Here, we demonstrate that lomitapide can directly bind to PP2A, and more importantly, PP2A knockout significantly abrogates the effect of lomitapide on AMPK phosphorylation and its downstream proteins in CRC cells, indicating that the regulation of AMPK phosphorylation by lomitapide is partially dependent on PP2A (Fig. 5). Moreover, lomitapide does not exert its anticancer effect in PP2A-deficient CRC cells (Fig. 6). Herein, we discovered that lomitapide may directly impair PP2A-mediated AMPK inactivation, leading to autophagic CRC cell death. Notably, more than 300 substrates can be dephosphorylated by PP2A [51], and whether other molecules are involved in the therapeutic mechanisms of lomitapide warrants further investigation.

Colorectal cancer (CRC) is among the most lethal and prevalent malignancies worldwide; it accounted for nearly 935,000 cancer-related deaths in 2020 [56]. After decades of development, great efforts have been devoted to updating CRC therapeutic drugs for better patient responses, fewer adverse events and more individualized treatment strategies. However, these regimens exhibit compromised clinical outcomes due to side effects or drug resistance, and the overall prognosis for CRC patients remains poor [57]. Therefore, the identification of novel targets and the renewal of effective drugs are in great demand for CRC patients. In summary, the current findings demonstrate that lomitapide suppresses CRC growth via induction of AMPK/Beclin1-mediated autophagic cell death by directly targeting PP2A without observed side effects. These data shed light on the therapeutic targets and mechanism of action of lomitapide and suggest the potential application of lomitapide in the management of CRC.

Conclusions

Our findings demonstrate that Lomitapide could inhibit CRC by inducing AMPK-dependent autophagy, and lomitapide could directly impair PP2A-regulated AMPK dephosphorylation while phosphorylated AMPK participates in the direct phosphorylation of Beclin1, contributing to enhanced binding of Beclin1 with pro-autophagic proteins such as Vps34 and Atg14, and leading to autophagic CRC cell death (Fig. 6i). Our study provides a preclinical rationale for development of lomitapide in the future treatment of CRC.

Abbreviations

CRC
Colorectal cancer
FDA
Food and Drug Administration
MTP
Mitochondrial trifunctional protein
MTOR
mammalian target of rapamycin
AMPK
AMP-activated protein kinase
MAPK
Mitogen-activated protein kinase
DARTS
Drug affinity responsive target stability
ARF1
ADP-ribosylation factor 1
LiP-SMap
limited proteolysis-mass spectrometry
PP2A
protein phosphatase 2A
ROS
Reactive oxygen species
ACC
acetyl-CoA carboxylase
ATG14
autophagy related 14
TUNEL
terminal deoxynucleotidyl transferase dUTP nick end labeling

Declarations

Ethics approval and consent to participate

Not applicable.

Consent for publication

All the authors agree to publish this paper.

Availability of data and material

The datasets used and/or analyzed during the current study are available from the corresponding author on reasonable request.

Competing interests

The authors declare no conflict of interest.

Funding

This research was supported by National Key R&D Program of China (2017YFA0505100), National Natural Sciences Foundation of China (82073196, 81803551, 31770888), Guangdong Natural Science Research Grant International joint project (2021A0505030035), Guangdong Natural Science Research Grant (2021A1515011158, 2020A1515110760), and the Fundamental Research Funds for the Central Universities (21620429).

Authors' contributions

Qian Zuo and Wen Wen Xu conceived the project. Wen Wen Xu, Qian Zuo, Long Liao, Zi Ting Yao and Ya Ping Liu designed the experiments and secured funding. Qian Zuo, Ding Kang Wang, Shu Jun Li performed the experiments. Qian Zuo and Zi Ting Yao analyzed the data. Qian Zuo and Ya Ping Liu wrote the manuscript. Wen Wen Xu provided editing and final approval of the manuscript.

Acknowledgements

Not applicable.

References

1. Bhandari A, Woodhouse M, Gupta S. Colorectal cancer is a leading cause of cancer incidence and mortality among adults younger than 50 years in the USA: a SEER-based analysis with comparison to other young-onset cancers. J Investig Med. 2017;65:311–5.
2. Goulooze SC, Cohen AF, Rissmann R. Lomitapide. Br J Clin Pharmacol. 2015;80:179–81.

3. Netea-Maier RT, Plantinga TS, van de Veerdonk FL, Smit JW, Netea MG. Modulation of inflammation by autophagy: Consequences for human disease. Autophagy. 2016;12:245–60.
4. Zhan Y, Gong K, Chen C, Wang H, Li W. P38 MAP kinase functions as a switch in MS-275-induced reactive oxygen species-dependent autophagy and apoptosis in human colon cancer cells. Free Radic Biol Med. 2012;53:532–43.
5. Strohecker AM, Guo JY, Karsli-Uzunbas G, Price SM, Chen GJ, Mathew R, et al. Autophagy sustains mitochondrial glutamine metabolism and growth of BrafV600E-driven lung tumors. Cancer discovery. 2013;3:1272–85.
6. Barrett JC, Hansoul S, Nicolae DL, Cho JH, Duerr RH, Rioux JD, et al. Genome-wide association defines more than 30 distinct susceptibility loci for Crohn's disease. Nat Genet. 2008;40:955–62.
7. Morselli E, Galluzzi L, Kepp O, Vicencio JM, Criollo A, Maiuri MC, et al. Anti- and pro-tumor functions of autophagy. Biochim Biophys Acta. 2009;1793:1524–32.
8. He S, Zhao Z, Yang Y, O'Connell D, Zhang X, Oh S, et al. Truncating mutation in the autophagy gene UVRAG confers oncogenic properties and chemosensitivity in colorectal cancers. Nat Commun. 2015;6:7839.
9. Moloney JN, Cotter TG. ROS signalling in the biology of cancer. Semin Cell Dev Biol. 2018;80:50–64.
10. Avalos Y, Canales J, Bravo-Sagua R, Criollo A, Lavandero S, Quest AF. Tumor suppression and promotion by autophagy. Biomed Res Int 2014; 2014: 603980.
11. Koustas E, Papavassiliou AG, Karamouzis MV. The role of autophagy in the treatment of BRAF mutant colorectal carcinomas differs based on microsatellite instability status. PLoS One. 2018;13:e0207227.
12. You P, Wu H, Deng M, Peng J, Li F, Yang Y. Brevilin A induces apoptosis and autophagy of colon adenocarcinoma cell CT26 via mitochondrial pathway and PI3K/AKT/mTOR inactivation. Biomed Pharmacother. 2018;98:619–25.
13. Meijer AJ, Lorin S, Blommaart EF, Codogno P. Regulation of autophagy by amino acids and MTOR-dependent signal transduction. Amino Acids. 2015;47:2037–63.
14. Wang Y, Zhang J, Li B, He QY. Advances of Proteomics in Novel PTM Discovery: Applications in Cancer Therapy. Small Methods 2019; 3.
15. Hu HF, Xu WW, Li YJ, He Y, Zhang WX, Liao L, et al. Anti-allergic drug azelastine suppresses colon tumorigenesis by directly targeting ARF1 to inhibit IQGAP1-ERK-Drp1-mediated mitochondrial fission. Theranostics. 2021;11:1828–44.
16. Piazza I, Kochanowski K, Cappelletti V, Fuhrer T, Noor E, Sauer U, et al. A Map of Protein-Metabolite Interactions Reveals Principles of Chemical Communication. Cell 2018; 172: 358 – 72 e23.
17. Mazhar S, Taylor SE, Sangodkar J, Narla G. Targeting PP2A in cancer: Combination therapies. Biochim Biophys Acta Mol Cell Res. 2019;1866:51–63.
18. Chang KE, Wei BR, Madigan JP, Hall MD, Simpson RM, Zhuang Z, et al. The protein phosphatase 2A inhibitor LB100 sensitizes ovarian carcinoma cells to cisplatin-mediated cytotoxicity. Mol Cancer

Ther. 2015;14:90–100.

19. Wei D, Parsels LA, Karnak D, Davis MA, Parsels JD, Marsh AC, et al. Inhibition of protein phosphatase 2A radiosensitizes pancreatic cancers by modulating CDC25C/CDK1 and homologous recombination repair. Clin Cancer Res. 2013;19:4422–32.
20. Dai C, Zhang X, Xie D, Tang P, Li C, Zuo Y, et al. Targeting PP2A activates AMPK signaling to inhibit colorectal cancer cells. Oncotarget. 2017;8:95810–23.
21. Cheng X, Shen D, Samie M, Xu H. Mucolipins. Intracellular TRPML1-3 channels. FEBS Lett. 2010;584:2013–21.
22. Huang XH, Wang Y, Hong P, Yang J, Zheng CC, Yin XF, et al. Benzethonium chloride suppresses lung cancer tumorigenesis through inducing p38-mediated cyclin D1 degradation. Am J Cancer Res. 2019;9:2397–412.
23. Wang Y, Zhang J, Huang ZH, Huang XH, Zheng WB, Yin XF, et al. Isodeoxyelephantopin induces protective autophagy in lung cancer cells via Nrf2-p62-keap1 feedback loop. Cell Death Dis. 2017;8:e2876.
24. Yang J, Xu WW, Hong P, Ye F, Huang XH, Hu HF, et al. Adefovir dipivoxil sensitizes colon cancer cells to vemurafenib by disrupting the KCTD12-CDK1 interaction. Cancer Lett. 2019;451:79–91.
25. Galluzzi L, Bravo-San Pedro JM, Levine B, Green DR, Kroemer G. Pharmacological modulation of autophagy: therapeutic potential and persisting obstacles. Nat Rev Drug Discov. 2017;16:487–511.
26. Ishaq M, Ojha R, Sharma AP, Singh SK. Autophagy in cancer: Recent advances and future directions. Semin Cancer Biol. 2020;66:171–81.
27. Grumati P, Coletto L, Sabatelli P, Cescon M, Angelin A, Bertaggia E, et al. Autophagy is defective in collagen VI muscular dystrophies, and its reactivation rescues myofiber degeneration. Nature medicine. 2010;16:1313–20.
28. Soubannier V, McLelland GL, Zunino R, Braschi E, Rippstein P, Fon EA, et al. A vesicular transport pathway shuttles cargo from mitochondria to lysosomes. Curr Biol. 2012;22:135–41.
29. Shen QW, Zhu MJ, Tong J, Ren J, Du M. Ca2+/calmodulin-dependent protein kinase kinase is involved in AMP-activated protein kinase activation by alpha-lipoic acid in C2C12 myotubes. Am J Physiol Cell Physiol. 2007;293:C1395-403.
30. Toyama EQ, Herzig S, Courchet J, Lewis TL Jr, Loson OC, Hellberg K, et al. Metabolism. AMP-activated protein kinase mediates mitochondrial fission in response to energy stress. Science. 2016;351:275–81.
31. Hinchy EC, Gruszczyk AV, Willows R, Navaratnam N, Hall AR, Bates G, et al. Mitochondria-derived ROS activate AMP-activated protein kinase (AMPK) indirectly. J Biol Chem. 2018;293:17208–17.
32. Kim J, Kim YC, Fang C, Russell RC, Kim JH, Fan W, et al. Differential regulation of distinct Vps34 complexes by AMPK in nutrient stress and autophagy. Cell. 2013;152:290–303.
33. Zhang D, Wang W, Sun X, Xu D, Wang C, Zhang Q, et al. AMPK regulates autophagy by phosphorylating BECN1 at threonine 388. Autophagy. 2016;12:1447–59.

34. Liu CY, Huang TT, Chen YT, Chen JL, Chu PY, Huang CT, et al. Targeting SET to restore PP2A activity disrupts an oncogenic CIP2A-feedforward loop and impairs triple negative breast cancer progression. EBioMedicine. 2019;40:263–75.
35. Galluzzi L, Pietrocola F, Bravo-San Pedro JM, Amaravadi RK, Baehrecke EH, Cecconi F, et al. Autophagy in malignant transformation and cancer progression. EMBO J. 2015;34:856–80.
36. He C, Klionsky DJ. Regulation mechanisms and signaling pathways of autophagy. Annu Rev Genet. 2009;43:67–93.
37. Abreu MM, Sealy L. The C/EBPbeta isoform, liver-inhibitory protein (LIP), induces autophagy in breast cancer cell lines. Exp Cell Res. 2010;316:3227–38.
38. Bai C, Zhang Z, Zhou L, Zhang HY, Chen Y, Tang Y. Repurposing Ziyuglycoside II Against Colorectal Cancer via Orchestrating Apoptosis and Autophagy. Front Pharmacol. 2020;11:576547.
39. Sun X, Yan P, Zou C, Wong YK, Shu Y, Lee YM, et al. Targeting autophagy enhances the anticancer effect of artemisinin and its derivatives. Med Res Rev. 2019;39:2172–93.
40. Uwe Nierbauer K, Paule J, Zizka G. Heteroploid reticulate evolution and taxonomic status of an endemic species with bicentric geographical distribution. AoB Plants 2017.
41. Kwitkowski VE, Prowell TM, Ibrahim A, Farrell AT, Justice R, Mitchell SS, et al. FDA approval summary: temsirolimus as treatment for advanced renal cell carcinoma. Oncologist. 2010;15:428–35.
42. Kumar R, Kapoor A. Current management of metastatic renal cell carcinoma: evolving new therapies. Curr Opin Support Palliat Care. 2017;11:231–7.
43. Redmann M, Benavides GA, Berryhill TF, Wani WY, Ouyang X, Johnson MS, et al. Inhibition of autophagy with bafilomycin and chloroquine decreases mitochondrial quality and bioenergetic function in primary neurons. Redox Biol. 2017;11:73–81.
44. Cha Y, Erez T, Reynolds IJ, Kumar D, Ross J, Koytiger G, et al. Drug repurposing from the perspective of pharmaceutical companies. Br J Pharmacol. 2018;175:168–80.
45. Ferreira LG, Andricopulo AD. Drug repositioning approaches to parasitic diseases: a medicinal chemistry perspective. Drug Discov Today. 2016;21:1699–710.
46. Joshi SN, Murphy EA, Olaniyi P, Bryant RJ. The multiple effects of aspirin in prostate cancer patients. Cancer Treat Res Commun. 2021;26:100267.
47. Huang XH, Yan X, Zhang QH, Hong P, Zhang WX, Liu YP, et al. Direct targeting of HSP90 with daurisoline destabilizes beta-catenin to suppress lung cancer tumorigenesis. Cancer Lett. 2020;489:66–78.
48. Xu WW, Huang ZH, Liao L, Zhang QH, Li JQ, Zheng CC, et al. Direct Targeting of CREB1 with Imperatorin Inhibits TGFbeta2-ERK Signaling to Suppress Esophageal Cancer Metastasis. Adv Sci (Weinh). 2020;7:2000925.
49. Hong-Brown LQ, Brown CR, Navaratnarajah M, Lang CH. FoxO1-AMPK-ULK1 Regulates Ethanol-Induced Autophagy in Muscle by Enhanced ATG14 Association with the BECN1-PIK3C3 Complex.

Alcohol Clin Exp Res. 2017;41:895–910.

50. Song X, Zhu S, Chen P, Hou W, Wen Q, Liu J, *et al*. AMPK-Mediated BECN1 Phosphorylation Promotes Ferroptosis by Directly Blocking System Xc(-) Activity. Curr Biol 2018; 28: 2388-99 e5.
51. Wlodarchak N, Xing Y. PP2A as a master regulator of the cell cycle. Crit Rev Biochem Mol Biol. 2016;51:162–84.
52. O'Connor CM, Perl A, Leonard D, Sangodkar J, Narla G. Therapeutic targeting of PP2A. Int J Biochem Cell Biol. 2018;96:182–93.
53. Saraf A, Oberg EA, Strack S. Molecular determinants for PP2A substrate specificity: charged residues mediate dephosphorylation of tyrosine hydroxylase by the PP2A/B' regulatory subunit. Biochemistry. 2010;49:986–95.
54. Zhu XN, Chen LP, Bai Q, Ma L, Li DC, Zhang JM, et al. PP2A-AMPKalpha-HSF1 axis regulates the metal-inducible expression of HSPs and ROS clearance. Cell Signal. 2014;26:825–32.
55. Yu HC, Lin CS, Tai WT, Liu CY, Shiau CW, Chen KF. Nilotinib induces autophagy in hepatocellular carcinoma through AMPK activation. J Biol Chem. 2013;288:18249–59.
56. Sung H, Ferlay J, Siegel RL, Laversanne M, Soerjomataram I, Jemal A, et al. Global cancer statistics 2020: GLOBOCAN estimates of incidence and mortality worldwide for 36 cancers in 185 countries. CA Cancer J Clin 2021.
57. El-Shami K, Oeffinger KC, Erb NL, Willis A, Bretsch JK, Pratt-Chapman ML, et al. American Cancer Society Colorectal Cancer Survivorship Care Guidelines. CA Cancer J Clin. 2015;65:428–55.

Figures

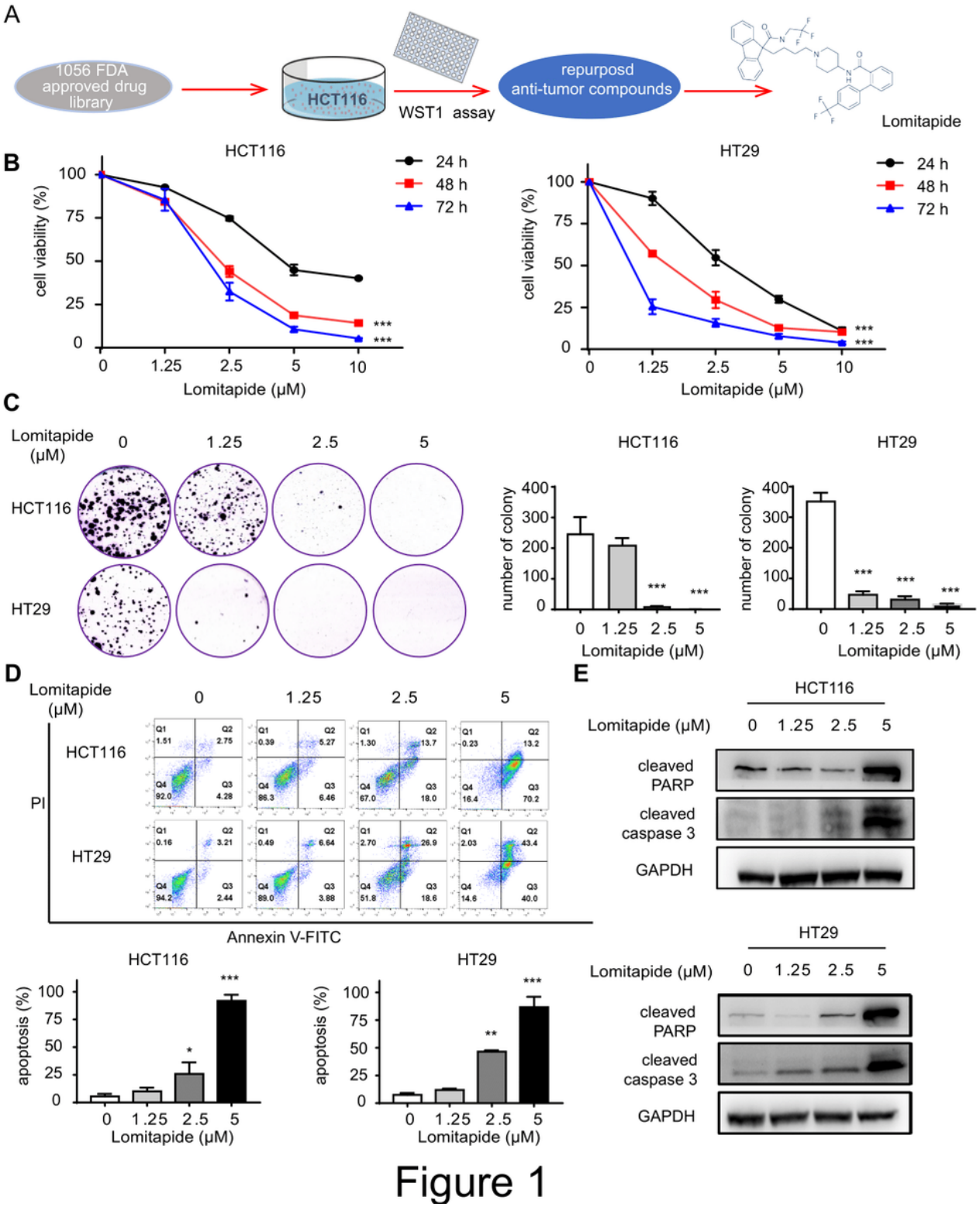

Figure 1

Figure 1

Screening of a FDA-approved small-molecule library led to the identification of lomitapide as a novel CRC anticancer compound. a Flow chart for the FDA-approved drug library screening used to identify compounds with CRC anticancer activities. b, c HCT116 and HT29 cells were treated with the indicated concentrations of lomitapide. Cell viability was assessed by WST-1 assay (b). Cell tumorigenesis was determined by colony formation (c). d, e Cells were treated with the indicated concentrations of

lomitapide for 48 h, apoptotic cells were analyzed by Annexin V-FITC/PI double-staining (d), and cleaved caspase-3 and cleaved PARP expression levels were compared (e). All the data are presented as the means±SD. *P < 0.05, **P < 0.01, ***P < 0.001.

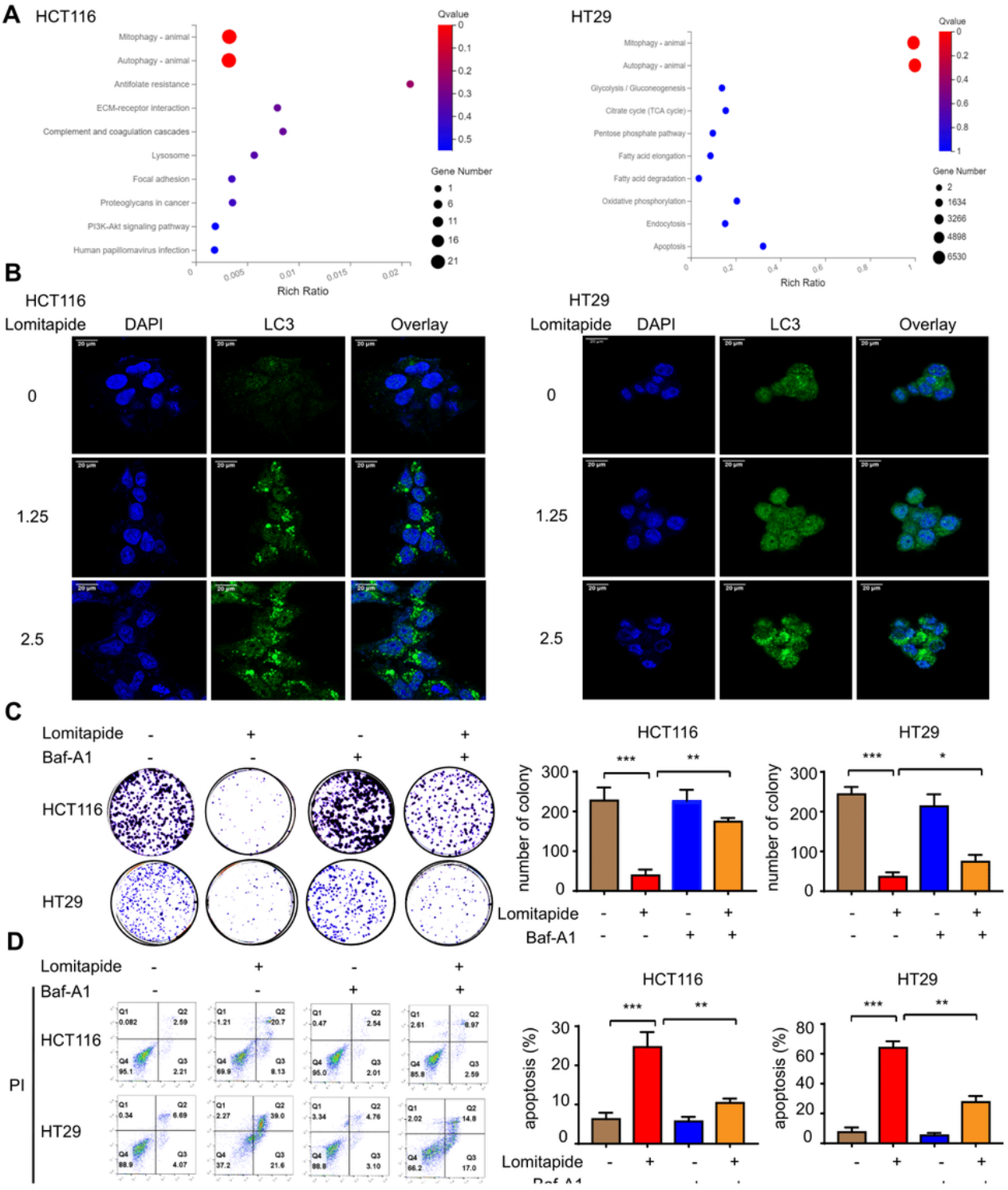

Figure 2

Figure 2

Autophagy induction contributes to the antitumor activity of lomitapide in CRC cells. a Identification of lomitapide-regulated biological process by bioinformatics analysis. b The accumulation of endogenous

LC3 puncta was quantitated by immunofluorescent analysis in the absence or presence of the indicated concentrations of lomitapide for 48 h. c HCT116 and HT29 cells were treated with Baf-A1 (0.5 nM) in the presence or absence of lomitapide (2.5 μM) for 48 h. Cell tumorigenesis was determined by colony formation. d The apoptotic effects induced by lomitapide were analyzed by Annexin V-FITC/PI double-staining. All the data are presented as the means±SD. *P < 0.05, **P < 0.01, ***P < 0.001.

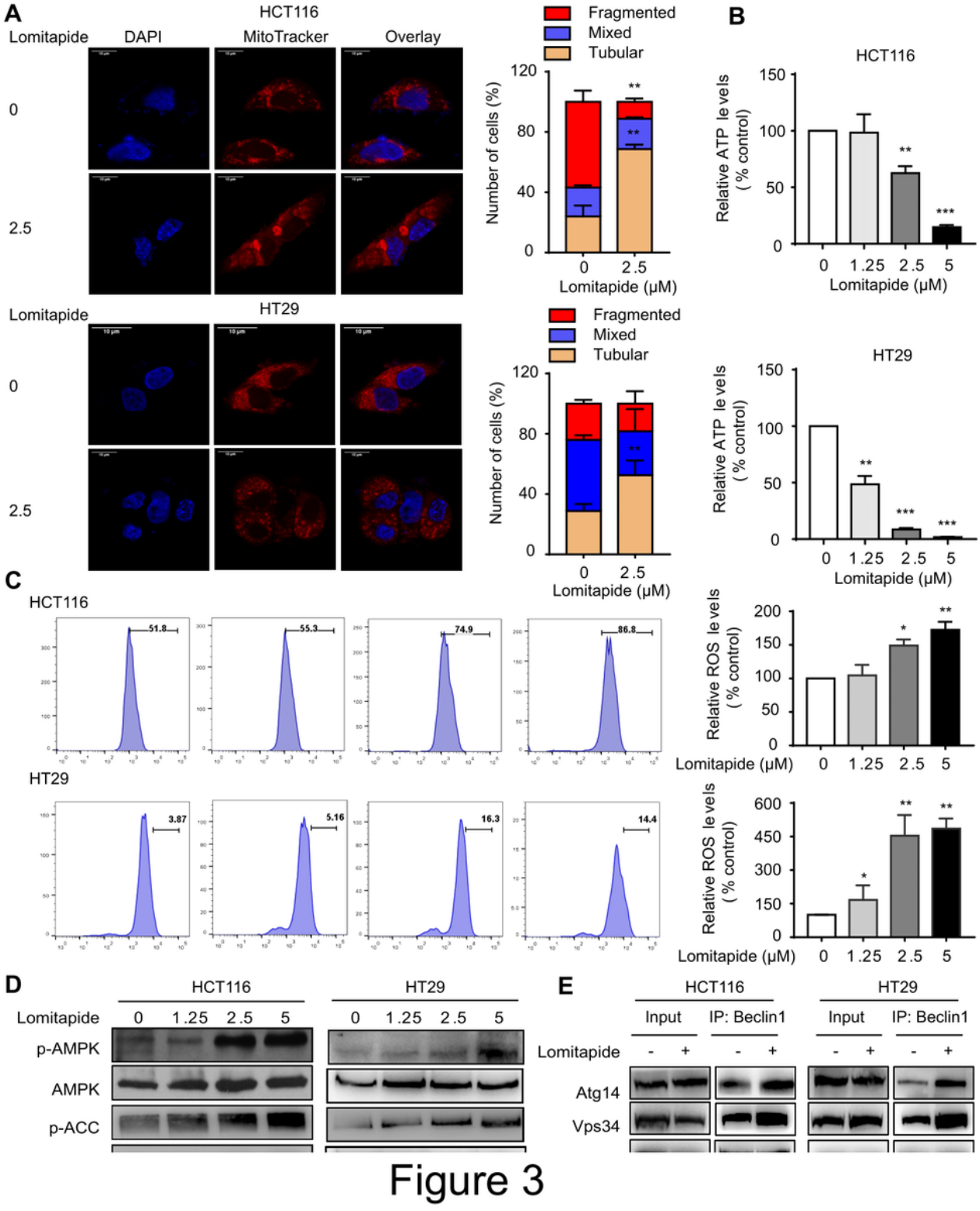

Figure 3

Lomitapide triggers AMPK-regulated autophagy through mitochondrial ATP depletion and ROS accumulation in CRC cells. a HCT116 cells and HT29 cells were treated with indicated concentrations of lomitapide for 48 h. Colocalization of blue DAPI puncta and MitoTracker red was observed by confocal microscopy, and it was quantified through the determination of altered mitochondrial morphology. b Intracellular ATP levels were detected by bioluminescence assay. c Intracellular ROS levels were evaluated by DHE assay. d Immunoblot analysis of AMPK, p-AMPK, and p-ACC expression in HCT116 and HT29 cells. e The interaction of Beclin1 with Vps34 or ATG14 after lomitapide treatment was determined by coimmunoprecipitation assay. All the data are presented as the means±SD. *P < 0.05, **P < 0.01, ***P < 0.001.

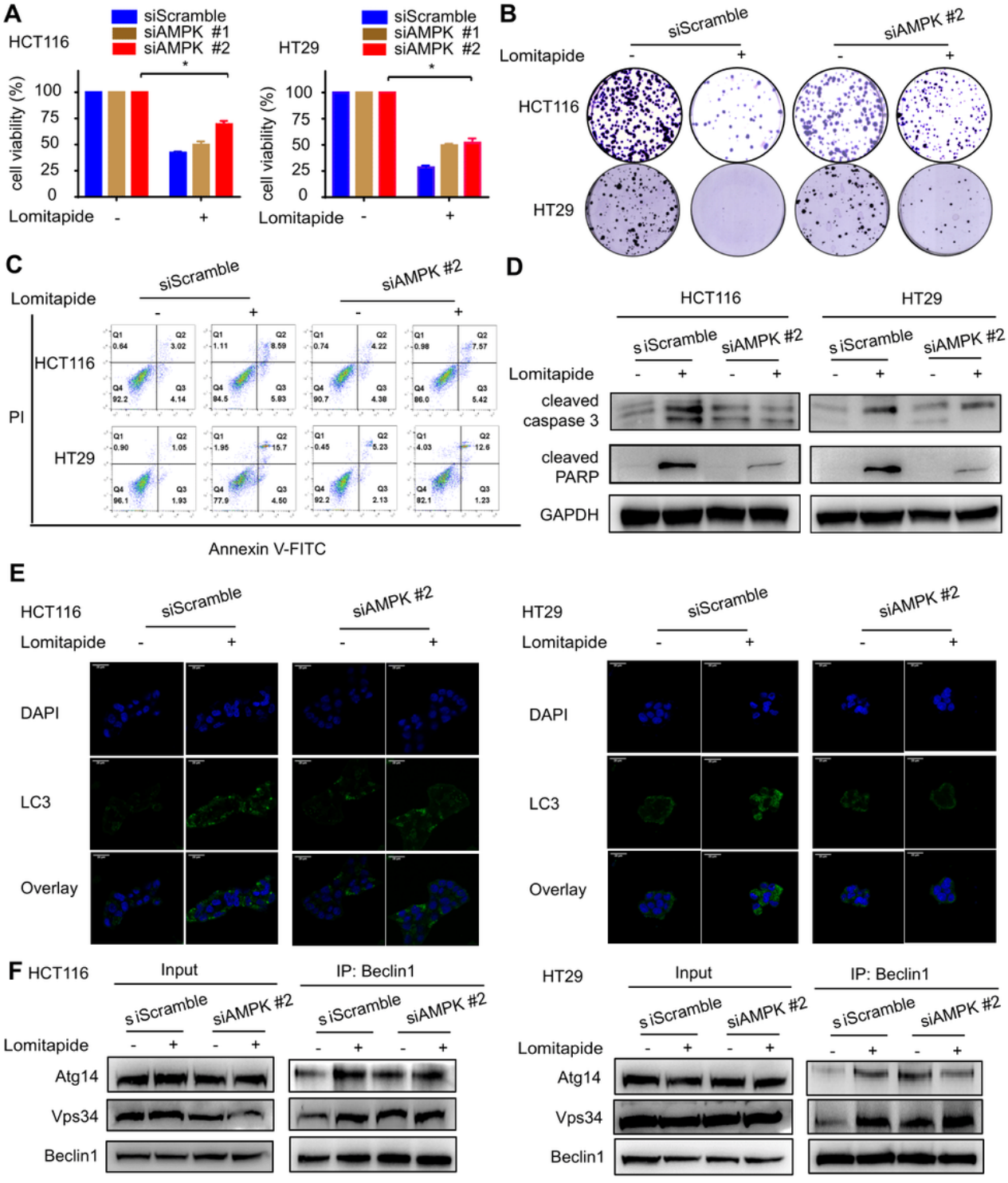

Figure 4

Figure 4

AMPK silencing prevents lomitapide-induced autophagic cell death. a HCT116 and HT29 cells were treated with siScramble or siAMPK in the presence or absence of lomitapide (2.5 μM) for 48 h. b-d Cells were treated as in a. Cell tumorigenesis was detected by colony formation (b). Apoptotic cells were analyzed by Annexin V-FITC/PI double-staining (c) and cleaved caspase-3 and cleaved PARP expression levels were compared (d). e, f Cells were treated as in a. The accumulation of endogenous LC3 puncta

was quantitated by immunofluorescent analysis in the absence or presence of lomitapide (e). The interaction of Beclin1 with Vps34 or Atg14 was determined by coimmunoprecipitation assay (f). All the data are presented as the means±SD. *P < 0.05, **P < 0.01, ***P < 0.001.

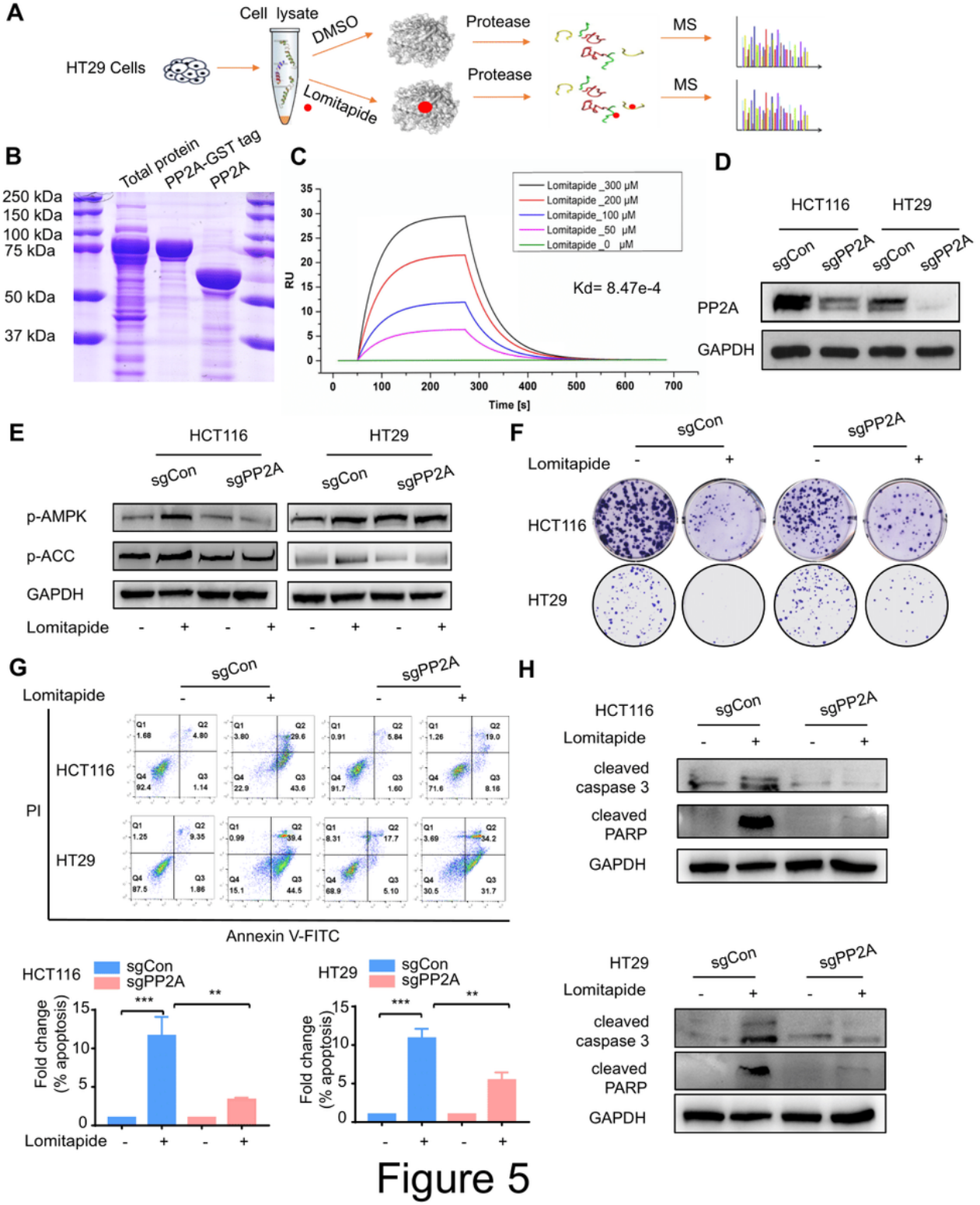

Figure 5

Figure 5

Targeting PP2A decreases lomitapide-induced AMPK phosphorylation and CRC suppression. a Flow chart depicting the LiP-SMap assay. Freshly prepared whole-cell lysates were treated with or without lomitapide

for 48 h, followed by proteinase K (PK) digestion and analysis by MS. The binding of lomitapide prevents PK digestion, leading to a differential MS peptide profile. More than 48,000 quantified peptides were identified, and this dataset was imported into the power law global error model (PLGEM) algorithm for further data analysis [17]. b, c SDS-PAGE results of total protein, PP2A-GST and PP2A as displayed by Coomassie brilliant blue staining (b). The interaction between PP2A and lomitapide was determined by representative surface plasmon resonance (SPR) sensorgram (c). d Immunoblots showing that PP2A was knocked out in the HCT116 and HT29 cells. e Immunoblots of p-ACC and p-AMPK in WT and PP2A-knockout CRC cells with or without lomitapide for 48 h. f-h WT and PP2A-knockout CRC cells were treated with vehicle or lomitapide for 48 h. Cell tumorigenesis was determined by colony formation (f). The apoptotic cell rate was analyzed by Annexin V-FITC/PI double-staining (g), and cleaved caspase-3 and cleaved PARP expression levels were compared (h). All the data are presented as the means±SD. *P < 0.05, **P < 0.01, ***P < 0.001.

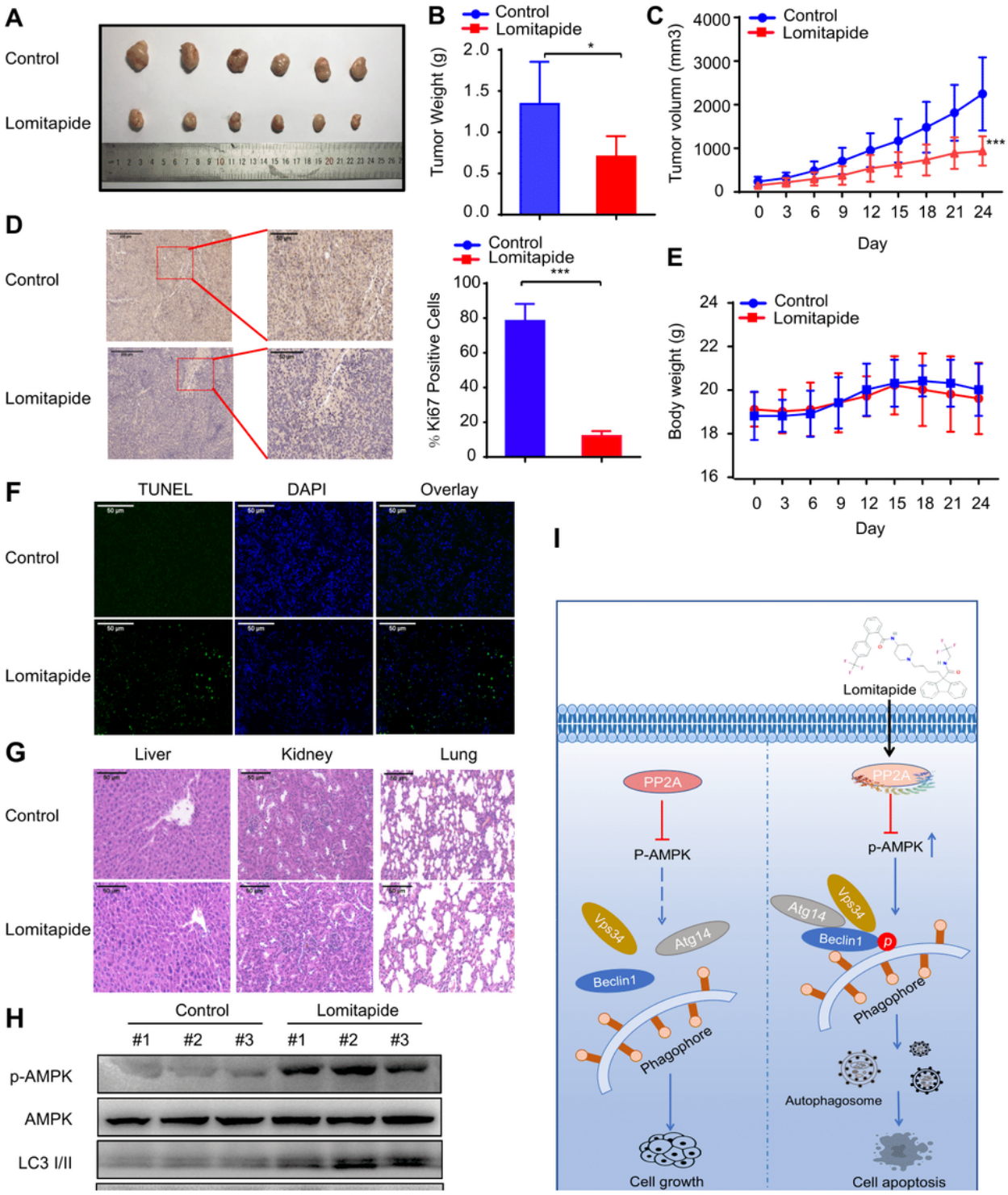

Figure 6

Figure 6

Lomitapide exhibits antitumor effect against CRC in vivo. Nude mice bearing HT29-derived tumor xenografts were orally administered 20 mg/kg lomitapide or vehicle every two days. a Image of the tumors. b Tumor weights. c Tumor growth curves showing that lomitapide exerted a significant inhibitory effect on the growth of the HT29-derived tumor xenografts (n = 6). d The Ki-67 immunohistochemistry results in the lomitapide-treatment and the vehicle groups were compared. e The body weights of the

nude mice during the experimental period. f The TUNEL assay results in the lomitapide-treatment and the vehicle groups were compared. g Hematoxylin and eosin (H&E) staining of the liver, kidney, and lung collected from the mice in the treatment and the vehicle groups. h Expression levels of AMPK, p-AMPK, LC3 I/II in the tumors from mice treated with lomitapide or vehicle were detected by Western blot. i Schematic diagram summarizing the mechanisms of action of lomitapide in CRC cells. All the data are presented as the means±SD. *P < 0.05, **P < 0.01, ***P < 0.001.

Supplementary Files

This is a list of supplementary files associated with this preprint. Click to download.

- supplementarymaterial.pdf